JOURNAL OF NATURAL PRODUCTS

pubs.acs.org/jnp

Article

Glyclauxins A−E: Dimeric Oxaphenalenone Aminoglycosides from an Australian Wasp Nest-Derived Fungus *Talaromyces* sp. CMB-MW102

Kaumadi Samarasekera, Waleed M. Hussein, Taizong Wu, Angela A. Salim, and Robert J. Capon*

Cite This: https://doi.org/10.1021/acs.jnatprod.2c01069

Read Online

ACCESS | Metrics & More | Article Recommendations | Supporting Information

ABSTRACT: Chemical analysis of cultures of a Queensland mud dauber wasp nest-derived fungus, *Talaromyces* sp. CMB-MW102, yielded the known dimeric oxaphenalenone duclauxin (**1**) along with a family of new 1-deoxy-D-glucosamine adducts, glyclauxins A−E (**2**−**6**). Despite 1D NMR spectra of **2**−**6** being compromised by broadening of selected resonances, structures inclusive of absolute configuration were assigned on the basis of detailed spectroscopic analysis and biogenetic considerations, as well as biomimetic semisynthesis and chemical interconversion. For example, exposure of duclauxin (**1**) to synthetic 1-deoxy-D-glucosamine yielded glyclauxin B (**3**), while on handling and storage, glyclauxins C (**4**) and D (**5**) (bearing a 7-OMe moiety) proved chemically labile and underwent quantitative transformation to glyclauxins B (**3**) and A (**2**), respectively. These latter observations on chemical reactivity and stability informed a proposed biogenetic relationship linking all known members of the extended duclauxin family. Notwithstanding their potential status as artifacts, the detection of glyclauxins B (**3**) and A (**2**) in a fresh CMB-MW102 culture extract confirmed their natural product status.

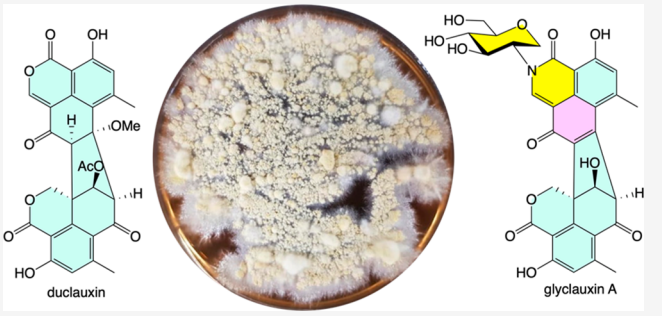

As part of our ongoing research into the chemical diversity of Australian microbes, we assembled a library of fungal and bacterial isolates from a mud dauber wasp sourced from an urban site near Brisbane. Preliminary investigations revealed several isolates to be adept at producing new natural products. These include the unprecedented nitro *depsi*-tetrapeptide diketopiperazine waspergillamide A from *Aspergillus* sp. CMB-W031[1] and siderophore diketopiperazine talarazines A−E from *Talaromyces* sp. CMB-W045[2] and the sulfated *p*-terphenyl talarophenol sulfate and azaphilone talarophilones A and B from *Talaromyces* sp. CMB-W045.[3] Building on this success we assembled a second library of fungal and bacterial isolates from a mud dauber wasp nest and demonstrated that these too were a source of new natural products, including an array of *anti* and *syn* bianthrone neobulgarones from *Penicillium* sp. CMB-MD22,[4] meroterpene oxandrastins from *Penicillium* sp. CMB-MD14,[5] and polyketide phoslactomycins, cyclolactomycins, and isocyclolactomycins from *Streptomyces* sp. CMB-MW079.[6] Continuing our investigations into mud dauber wasp nest-derived microbes, we applied a global natural products social (GNPS) molecular networking[7] workflow to better prioritize potentially new natural products. This approach drew attention to *Talaromyces* sp. CMB-MW102 as a source of natural products with unprecedented molecular formulas. Subsequent chemical fractionation yielded the known dimeric oxophenalenone duclauxin (**1**) along with five new deoxyaminosugar conjugates, glyclauxins A−E (**2**−**6**), with structures assigned by detailed spectroscopic and chemical analysis, as well as semisynthesis, chemical transformations, and biogenetic considerations.

RESULTS AND DISCUSSION

A GNPS molecular network analysis of a library of EtOAc extracts prepared from potato dextrose agar (PDA) cultures of 36 mud dauber wasp nest-derived fungi highlighted a molecular family unique to *Talaromyces* sp. CMB-MW102 (Figure S4) and inclusive of molecular formulas unprecedented in the natural product scientific literature. The EtOAc extract of a scaled-up (×100 plate) 14-day PDA cultivation was subjected to solvent partitioning and sequential trituration followed by reversed phase chromatography to yield **1**−**6**. Compound **1** was readily identified by detailed spectroscopic analysis and comparison with literature data as the known dimeric oxyphenalenone duclauxin (Table S1 and Figures S5−

Special Issue: Special Issue in Honor of Mary J. Garson

Received: November 24, 2022

Chart 1

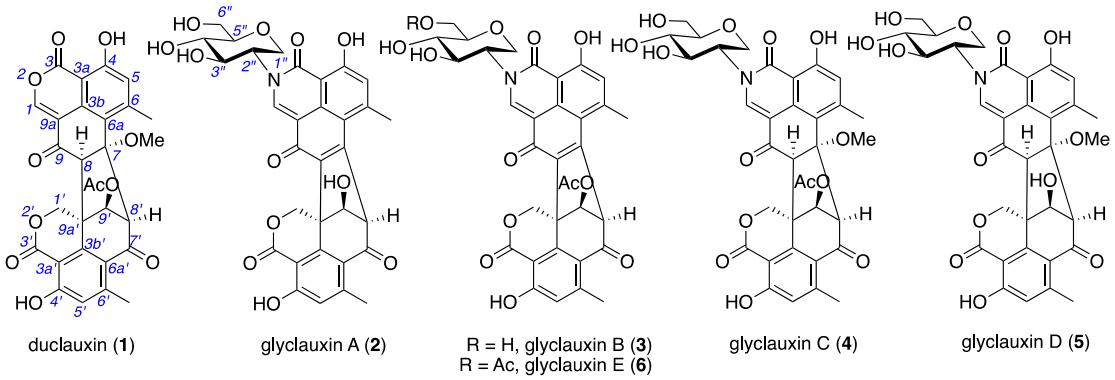

S7). First described in 1965 from *Penicillium duclauxii*,[8] **1** and related analogues have since been reported from multiple fungi of the genera *Penicillium* and *Talaromyces*,[9] with the structure originally assigned by spectroscopic analysis[8] and configurational assignments later proposed by X-ray crystallographic analysis on a monobromo derivative.[10] Curiously the latter assignment proved incorrect, with a 2015 X-ray analysis of the naturally occurring ethanolamine adduct duclauxamide A1 (**7**) prompting a revision from 9′*R* to 9′*S* (Figure 1).[11] Significantly, the co-metabolites **2**–**6** proved to be new exemplars of the duclauxin scaffold, and an account of their structure elucidation is outlined below.

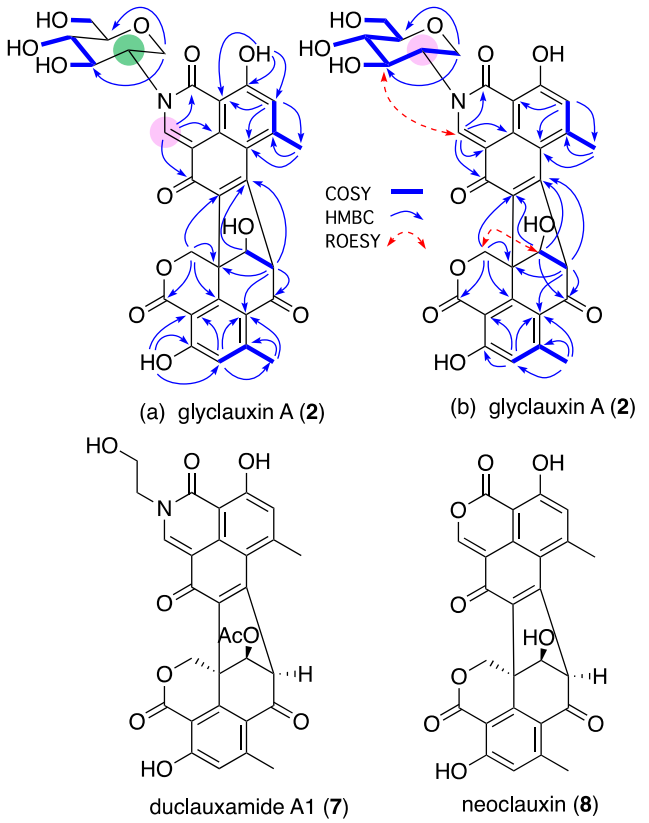

Figure 1. 2D NMR correlations for glyclauxin A (**2**) in (a) DMSO-d_6 and (b) pyridine-d_5 and structures for duclauxamide A1 (**7**) and neoclauxin (**8**). Highlights: both ^{1}H and ^{13}C NMR resonances not detected (green); only ^{13}C NMR resonances not detected (pink).

HRESIMS analysis of **2** revealed a molecular formula ($C_{32}H_{27}NO_{12}$, Δmmu −1.1) requiring 20 double-bond equivalents (DBE). Comparison of the NMR (DMSO-d_6) data for **2** (Tables 1, 2, and S2 and Figures 1a and S8–S12) with **1** revealed a high level of similarity, with key differences attributed to replacement of resonances for 7-OMe (δ_H 2.90, 7-OC$\underline{H}_3$; δ_C 51.4, 7-O$\underline{C}H_3$; 88.3, C-7), H/C-8 (δ_H 3.99, H-8; δ_C 63.2, C-8), and 9′-OAc (δ_H 5.20, H-9′; 2.17, 9′-OCO$\underline{C}H_3$;

Table 1. ^{1}H NMR (600 MHz, DMSO-d_6) Data for Glyclauxins A–C (2–4)

	glyclauxin A (**2**)	glyclauxin B (**3**)	glyclauxin C (**4**)
position	δ_H, mult. (J in Hz)	δ_H, mult. (J in Hz)	δ_H, mult. (J in Hz)
1	8.73, s	8.78, s	7.79, s
5	7.00, s	7.00, s	6.79, s
8			3.96, s
4-OH	12.95, s	12.97, s	12.46, s
6-Me	2.98, s	2.95, s	2.60, s
7-OMe			2.87, s
1′	*a.* 5.03, d (12.3)	*a.* 5.02, d (12.3)	*a.* 5.10, d (11.9)
	b. 4.85, d (12.3)	*b.* 4.91, d (12.3)	*b.* 4.97, d (11.9)
5′	6.83, q (0.7)	6.89, q (0.7)	6.60, s
8′	4.76, d (0.8)	4.93, d (0.8)	4.00, s
9′	4.69, br d (5.2)	5.75, d (0.8)	5.16, s
4′-OH	12.03, s	11.99, s	11.61, br s
6′-Me	2.51[a]	2.52, d (0.7)	1.92, s
9′-OH	6.35, d (5.2)		
9′-OCOC$\underline{H}_3$		2.02, s	2.17, s
1″	*a.* 3.89, dd (10.7, 4.8)	*a.* 3.88, dd (10.8, 4.9)	*a.* 3.71, dd (11.0, 4.5)
	b. 3.78, br s	*b.* 3.77, br s	*b.* n.o.
2″	n.o.[b]	n.o.	n.o.
3″	3.99, br s	3.99, br s	n.o.
4″	3.24, m	3.25, dd (9.2, 8.2)	3.21, m
5″	3.33[c]	3.33[c]	3.24, m
6″	*a.* 3.70, ddd (11.8, 5.3, 2.0)	*a.* 3.70, dd (11.9, 1.8)	*a.* 3.68, ddd (11.7, 5.9, 1.3)
	b. 3.47, ddd (11.8, 5.3, 5.3)	*b.* 3.47, dd (11.9, 5.9)	*b.* 3.45, ddd (11.7, 5.9, 5.9)
3″-OH	5.37, d (5.3)	n.o.	n.o.
4″-OH	5.26, d (5.3)	n.o.	5.26, d (4.9)
6″-OH	4.60, dd (5.3, 5.3)	n.o.	4.58, dd (5.9, 5.9)

[a]Partially obscured by DMSO signal. [b]n.o. not observed. [c]Partially obscured by H_2O signal.

https://doi.org/10.1021/acs.jnatprod.2c01069
J. Nat. Prod. XXXX, XXX, XXX−XXX

Table 2. ^{13}C NMR (150 MHz, DMSO-d_6) Data for Glyclauxins A−E (2−6)

position	(2) δ_C, type	(3) δ_C, type	(4) δ_C, type	(5) δ_C, type	(6) δ_C, type
1	n.o.[a]	n.o.	n.o	n.o	n.o.
3	165.4, C	165.7, C	165.5, C	165.6, C	165.2, C
3a	107.9, C	108.0, C	106.8, C	106.9, C	108.2, C
3b	134.0, C	134.3, C	134.3, C	134.4, C	134.5, C
4	163.5, C	163.9, C	160.6, C	160.5, C	n.o.
5	117.6, CH	117.7, CH	117.1, CH	117.1, CH	118.4, CH
6	148.6, C	149.0, C	148.0, C	147.9, C	148.8, C
6a	114.4, C	113.8, C	116.5, C	117.6, C	113.4, C
7	151.9, C	151.2, C	88.0, C	88.7, C	151.6, C
8	147.7, C	146.5, C	63.3, CH	63.2, CH	147.2, C
9	177.3, C	176.7, C	193.3, C	194.5, C	176.6, C
9a	113.8, C	113.6, C	111.2, C	111.7, C	114.0, C
6-Me	24.3, CH_3	24.1, CH_3	21.3, CH_3	21.3, CH_3	24.4, CH_3
7-OMe			51.2, CH_3	51.1, CH_3	
1′	69.3, CH_2	68.0, CH_2	70.6, CH_2	71.9, CH_2	67.8, CH_2
3′	167.8, C	167.3, C	166.5, C	167.1, C	166.6, C
3′a	104.3, C	104.3, C	105.4, C	105.5, C	105.0, C
3′b	139.7, C	139.5, C	143.3, C	144.2, C	138.8[b], C
4′	163.1, C	163.2, C	166.5, C	163.1, C	n.o.
5′	119.5, CH	120.0, CH	120.2, CH	119.6, CH	121.2, CH
6′	152.4, C	152.7, C	149.7, C	149.5, C	151.6, C
6′a	116.8, C	116.6, C	120.8, C	121.6, C	114.8[b], C
7′	191.6, C	190.2, C	191.4, C	193.4, C	190.0, C
8′	66.3, CH	62.8, CH	67.3, CH	71.0, CH	62.7, CH
9′	84.1, CH	83.7, CH	78.3, CH	77.8, CH	84.1, CH
9′a	49.2, C	48.0, C	51.2, C	53.0, C	47.9, C
6′-Me	23.2, CH_3	23.1, CH_3	21.4, CH_3	21.3, CH_3	23.3, CH_3
9′-OCO$\underline{C}H_3$		20.7, CH_3	20.8, CH_3		20.8, CH_3
9′-O$\underline{C}OCH_3$		170.2, C	169.7, C		170.2, C
1″	66.0, CH_2	66.0, CH_2	65.3, CH_2	65.4, CH_2	66.2, CH_2
2″	n.o.	n.o	n.o.	n.o	n.o
3″	72.6, CH	72.6, CH	n.o.	n.o	72.4, CH
4″	71.1, CH	71.0, CH	71.6, CH	71.6, CH	71.1, CH
5″	81.5, CH	81.4, CH	81.5, CH	81.6, CH	78.0, CH
6″	61.2, CH_2	61.1, CH_2	61.1, CH_2	61.2, CH_2	64.0, CH_2
6″-OCO$\underline{C}H_3$					20.8, CH_3
6″-O$\underline{C}OCH_3$					170.6, C

[a]n.o. not observed. [b]Detected from HMBC.

δ_C 78.3, C-9′; 20.7, 9′-OCO$\underline{C}H_3$; 169.6, 9′-O$\underline{C}OCH_3$) in **1** with resonances for a $\Delta^{7,8}$ (δ_C 151.9, C-7; 147.7, C-8) and 9′-OH (δ_H 4.69, H-9′; 6.35, 9′-OH; δ_C 84.1, C-9′) in **2**. Such structure differences were consistent with those previously reported for neoclauxin (**8**) (Figure 1), a base-catalyzed transformation product (artifact) of **1**.[12] This structure assignment was further confirmed by diagnostic 2D NMR (DMSO-d_6) correlations in **2** from both H-8′ and H-9′ to C-7 and from H_2-1′ to C-8. Another noteworthy difference in the NMR (DMSO-d_6) data was deshielding of H-1 in **2** (δ_H 8.73) compared to **1** (δ_H 7.91), suggestive of replacement of the isocoumarin moiety in **1** with an N-substituted 1(2*H*)-isoquinolinone moiety in **2**, in common with that observed in duclauxamide A1 (**7**).[11] A curiosity in the NMR (DMSO-d_6) data for **2** was the inability to detect the C-1 resonance, even though this resonance was clearly detectable in the NMR (DMSO-d_6) data for **1** (δ_C 149.6). By contrast, analysis of the NMR (pyridine-d_5) data for **2** (Table S3 and Figures 2b and S13−S18) revealed C-1 (δ_C 140.6). Based on the above, the unassigned $C_6H_{11}O_4$ structure fragment in **2** must be pendant to N-2 and feature one DBE, with the 1D NMR (DMSO-d_6) data requiring an oxymethylene (δ_H 3.78/3.89, C$\underline{H}_2$O; δ_C 66.0, $\underline{C}H_2O$), an oxymethine (δ_H 3.33, C$\underline{H}$O; δ_C 81.5, $\underline{C}$HO), a hydroxymethylene (δ_H 3.47/3.70, C$\underline{H}_2$OH; 4.60, CH$_2$O$\underline{H}$; δ_C 61.2, $\underline{C}H_2OH$), and two hydroxymethines (δ_H 3.99, C$\underline{H}$OH; 5.37, CHO$\underline{H}$; δ_C 72.6, $\underline{C}$HOH; and δ_H 3.24, C$\underline{H}$OH; 5.26, CHO$\underline{H}$; δ_C 71.1, $\underline{C}$HOH) with undetectable resonances for the remaining CH moiety (Figure 1a), necessitating an oxy-heterocycle. Analysis of the NMR (pyridine-d_5) data for **2** revealed all proton resonances and supported by 2D COSY correlations allowed assembly of a remaining structure fragment as a 1-deoxyglucosamine moiety (Figure 1b), with the relative configuration evident from diagnostic axial−axial *J* coupling ($J_{1''ax,2''}$ 10.9 Hz; $J_{2'',3''}$ 8.6 Hz; $J_{3'',4''}$ 8.6 Hz; $J_{4'',5''}$ 9.4 Hz). Curiously, the ^{13}C NMR resonance for C-2″ remained undetectable in either DMSO-d_6 or pyridine-d_5. These observations together with biogenetic considerations permitted assignment of the structure for glyclauxin A (**2**) as shown.

HRESIMS analysis of **3** revealed a molecular formula ($C_{34}H_{29}NO_{13}$, Δmmu −1.1) consistent with an acetyl homologue of **2**. Comparison of the 1D NMR (DMSO-d_6) data for **3** (Tables 1, 2, and S4 and Figures S20 and S21) with

https://doi.org/10.1021/acs.jnatprod.2c01069
J. Nat. Prod. XXXX, XXX, XXX−XXX

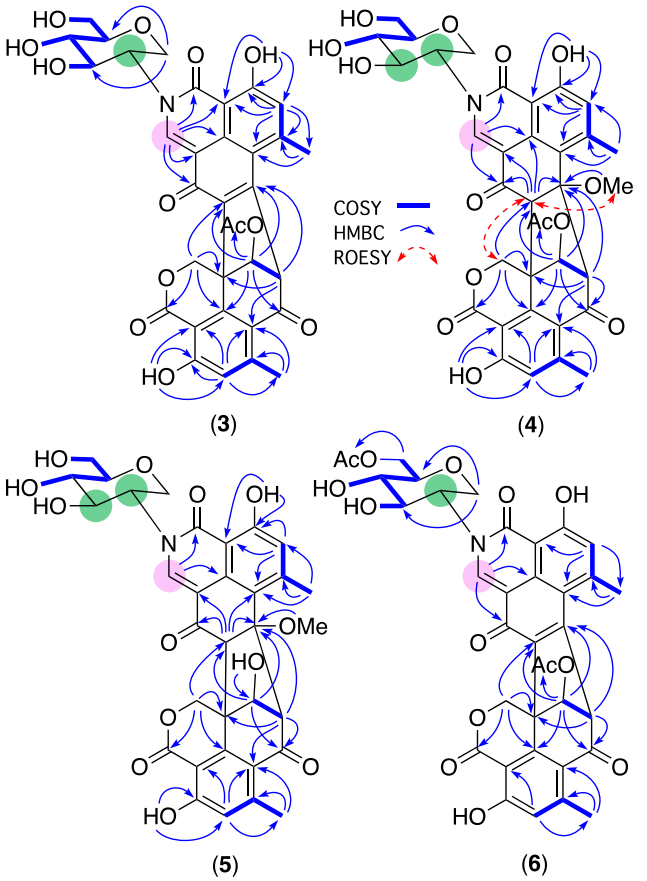

Figure 2. 2D NMR (DMSO-d_6) correlations for glyclauxins B–E (**3**–**6**). Highlights: both ^{1}H and ^{13}C NMR resonances not detected (green); only ^{13}C NMR resonances not detected (pink).

those of **2** showed significant similarities, including an inability to detect resonances for C-1, C-2″, and H-2″, with the key differences attributed to conversion of the 9′-OH in **2** (δ_H 4.69, H-9′; 6.35, 9′-O<u>H</u>; δ_C 84.1, C-9′) to a 9′-OAc moiety in **3** (δ_H 2.02, 9′-OCOC<u>H</u>$_3$; δ_C 20.7, 9′-OCO<u>C</u>H$_3$; 170.2, 9′-O<u>C</u>OCH$_3$). Together with diagnostic 2D NMR correlations (Figures 2 and S22–S24) and biogenetic considerations, the structure for glyclauxin B (**3**) was assigned as shown.

HRESIMS analysis of **4** revealed a molecular formula ($C_{35}H_{33}NO_{14}$, Δmmu −0.2) consistent with a MeOH addition homologue of **3**. Comparison of the 1D NMR (DMSO-d_6) data for **4** (Tables 1, 2, and S5 and Figures S26 and S27) with those of **3** showed significant similarities, including an inability to detect resonances for C-1, C-2″, and H-2″ (as well C-3″ and H-3″), with key differences attributed to a C-7/C-8 substitution and configuration in **4** (δ_H 2.87, 7-OC<u>H</u>$_3$; δ_C 51.2, 7-O<u>C</u>H$_3$; 88.0, C-7; δ_H 3.96, H-8; δ_C 63.3, C-8) in common with **1** (δ_H 2.90, 7-OC<u>H</u>$_3$; δ_C 51.4, 7-O<u>C</u>H$_3$; 88.3, C-7; δ_H 3.99, H-8; δ_C 63.2, C-8). Together with diagnostic 2D NMR correlations (Figures 2 and S28–S30) and biogenetic considerations the structure for glyclauxin C (**4**) was assigned as shown.

HRESIMS analysis of **5** revealed a molecular formula ($C_{33}H_{31}NO_{13}$, Δmmu 4.0) consistent with a deacetyl homologue of **4**. Comparison of the 1D NMR (DMSO-d_6) data for **5** (Tables 2, 3, and S6 and Figures S32 and S33) with those of **4** showed significant similarities, including an inability to detect resonances for C-1, C-2″, C-3″, H-2″, and H-3″, with

Table 3. ^{1}H NMR (600 MHz, DMSO-d_6) Data for Glyclauxins D and E (5 and 6)

	glyclauxin D (**5**)	glyclauxin E (**6**)
position	δ_H, mult. (*J* in Hz)	δ_H, mult. (*J* in Hz)
1	7.74, s	8.76, s
5	6.76, s	6.92, s
8	3.93, s	
4-OH	12.43, s	
6-Me	2.62, s	2.93, s
7-OMe	2.83, s	
1′	*a*. 4.96, d (12.0)	*a*. 4.92, d (12.0)
	b. 4.94, d (12.0)	*b*. 4.84, d (12.0)
5′	6.54, s	6.70, s
8′	3.79, s	4.87, s
9′	4.17, d (4.1)	5.68, s
4′-OH	11.56, s	
6′-Me	1.89, s	2.45, s
9′-OH	6.32, d (4.1)	
9′-OCOC<u>H</u>$_3$		2.01, s
1″	*a*. 3.71, dd (10.7, 4.6)	*a*. 3.88, dd (10.8, 5.0)
	b. n.o.[a]	*b*. n.o.
2″	n.o.	n.o.
3″	n.o.	4.02, br d
4″	3.21, m	3.28, dd (8.7, 8.7)
5″	3.24, m	3.59[b]
6″	*a*. 3.69, m	*a*. 4.33, dd (11.8, 1.7)
	b. 3.45[b]	*b*. 4.05, dd (11.8, 5.9)
6″-OCOC<u>H</u>$_3$		2.04, s
3″-OH		5.49, br s
4″-OH	5.27, br s	5.56, br s
6″-OH	4.62, dd (5.9, 5.9)	

[a]n.o. not observed. [b]Partially obscured by H_2O.

the key differences attributed to conversion of the 9′-OAc in **4** (δ_H 5.16, H-9′; 2.17, 9′-OCOC<u>H</u>$_3$; δ_C 78.3, C-9′; 20.8, 9′-OCO<u>C</u>H$_3$; 169.7, 9′-O<u>C</u>OCH$_3$) to a 9′-OH in **5** (δ_H 4.17, H-9′; 6.32, 9′-O<u>H</u>; δ_C 77.8, C-9′). Together with diagnostic 2D NMR correlations (Figures 2 and S34–S36) and biogenetic considerations the structure for glyclauxin D (**5**) was assigned as shown.

HRESIMS analysis of **6** revealed a molecular formula ($C_{36}H_{31}NO_{14}$, Δmmu −1.2) consistent with an acetyl homologue of **3**. Comparison of the 1D NMR (DMSO-d_6) data for **6** (Tables 2, 3, and S7 and Figures S38 and S39) with **3** showed significant similarities, with the key differences attributed to conversion of the 6″-OH in **3** (δ_H 3.47/3.70, H$_2$-6″; δ_C 61.1, C-6″) to a 6″-OAc in **6** (δ_H 4.05/4.33, H$_2$-6″; 2.04, 6″-OCOC<u>H</u>$_3$; δ_C 64.0, C-6″; 20.8, 6″-OCO<u>C</u>H$_3$; 170.6, 6″-O<u>C</u>OCH$_3$). Together with diagnostic 2D NMR correlations (Figures 2 and S40–S42) and biogenetic considerations, the structure for glyclauxin E (**6**) was assigned as shown.

Given the anomalous broadening of selected 1D NMR resonances across **2**–**6**, we elected to provide supporting evidence by undertaking a biomimetic synthesis of glyclauxin B (**3**) starting from duclauxin (**1**). Prior to embarking on this, in a proof of concept study, a mixture of **1** and D-glucosamine was allowed to stand in DMSO at rt for 4 h, after which the solvent was removed *in vacuo* and the residue purified by HPLC to yield a single product, the D-glucosamine conjugate glyclauxin C1 (**9**) (Scheme 1). While the NMR (pyridine-d_5) data for **9** were consistent with the proposed structure, it did reveal partial conversion to the MeOH elimination product glyclauxin

https://doi.org/10.1021/acs.jnatprod.2c01069
J. Nat. Prod. XXXX, XXX, XXX−XXX

Scheme 1[a]

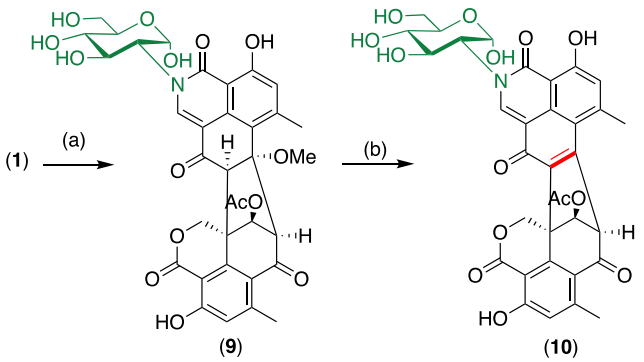

[a]Conditions: (a) D-glucosamine, DMSO, rt, 4 h, (b) pyridine-d_5, rt, 5 days.

B1 (**10**). Storage of this NMR sample at rt for 5 days led to quantitative conversion of **9** to **10** (Scheme 1), whose structure was confirmed by spectroscopic analysis (Table S8 and Figures S44−S48). This latter transformation was not unexpected, as on handling and storage glyclauxins C (**4**) and D (**5**) were observed to undergo the same MeOH elimination, with quantitative conversion to glyclauxins B (**3**) and A (**2**), respectively.

Next, we prepared a synthetic sample of authentic 1-deoxy-D-glucosamine HCl salt (**11**) (Scheme 2, Figures S55−S57) and repeated the adduct formation to transform **1** through glyclauxin C (**4**) to glyclauxin B (**3**), with the 1D NMR (DMSO-d_6) data for synthetic and natural **3** being identical (Figures S58 and S59). Significantly, correlation of the specific rotations for synthetic **3** ($[\alpha]_D$ −344) with natural **3** ($[\alpha]_D$ −374) permitted configurational assignment to the 1-deoxy-D-glucosamine residue in **2**−**6**. A likely mechanism for the reaction of 1-deoxy-D-glucosamine (and D-glucosamine) with duclauxin (**1**) proceeds via initial nucleophilic addition and ring opening of the C-3 lactone moiety followed by a Schiff base recyclization with concomitant loss of water (Figure 3).[13]

Interestingly, unlike the situation for all the natural product glyclauxins **2**−**6**, the NMR (pyridine-d_5 and DMSO-d_6) data (Figures S44, S45, S67, and S68) for the semisynthetic D-glucosamine adduct **10** revealed all the expected resonances and correlations and were fully consistent with the proposed structure. In an effort to understand this distinction, we noted that an energy-minimized model (Chem3D) of **10** supported the lowest energy conformation featuring a hydrogen bond between 1″-OH and O-3 (Figures 4 and S64). As this H-bond is not feasible for **2**−**6** (Figure S65), we postulate that NMR resonance broadening is associated with greater freedom of rotation, leading to a population of rotamers on an NMR time scale. We have previously observed the same phenomenon in fungal alkaloids belonging to the chrysosporazine family.[14]

Having documented the facile chemical transformation of glyclauxin C (**4**) to B (**3**), and D (**5**) to A (**2**), and forewarned by earlier experience that natural products can transform to artifacts during extraction, isolation, and/or handling,[15] we carried out analytical studies to confirm the natural product status of **1**−**6**. A PD broth culture of CMB-MW102 was carefully filtered to separate mycelia from culture broth, and both were separately extracted with EtOAc, dried under N_2 at rt, resuspended in MeOH, and immediately subjected to UPLC-DAD-MS analysis. These analyses successfully detected **1**−**6** in both the mycelia and culture broth, supportive of their status as natural products (Figure S62). Having synthesized **10**, we took this opportunity to repeat the GNPS analysis of the extract using **10** as a probe. This analysis confirmed that **10** coclusters with **2**−**5** and that no other nodes are detected (Figure S66). That is, there are no natural D-glucosamine glyclauxins in the *Talaromyces* sp. CMB-MW102.

Building on these observations, a plausible biogenetic relationship linking glyclauxins A−E (**2**−**6**) with duclauxin (**1**) (Scheme 3) would see (i) glyclauxin C (**4**) as a 1-deoxy-D-glucosamine (**11**) adduct of **1**, (ii) with glyclauxins D (**5**) and B (**3**) being acetate hydrolysis and MeOH elimination products of **4**, respectively, (iii) glyclauxin A (**2**) as either a MeOH elimination product of **5** and/or a deacetylation product of **3**, and (iv) glyclauxin E (**6**) as a acetylation product of **3**. Consistent with the relationship between glyclauxins, **1** has already been reported to readily and rapidly form amino acid adduct talauxins,[13] while duclauxamides A, B, and C might be viewed as naturally occurring ethanolamine, γ-aminobutyric acid, and methyl γ-aminobutyrate adducts[16] and bacillisporin H as an ammonia adduct of **1** (Scheme 3).[17] Given the reactivity of duclauxin, it is possible that some of these transformations occur nonenzymatically.

The metabolites **1**−**6** did not exhibit significant inhibition of the growth of human colon (SW620) or lung (NCI-H460) carcinoma cells (IC_{50} > 30 μM) (Figure S59) or the fungus *Candida albicans* ATCC10231, the Gram-negative bacterium *Escherichia coli* ATCC11775, or the Gram-positive bacteria *Staphylococcus aureus* ATCC25923 (IC_{50} > 30 μM).

In summary, a molecular network based strategy for natural product dereplication and prioritization detected the unprecedented glyclauxins A−E (**2**−**6**) in PD cultures of a Queensland mud dauber wasp nest-derived fungus, *Talaromyces* sp. CMB-MW102. Spectroscopic analysis of **2**−**6** revealed anomalous broadening of selected ^{1}H and ^{13}C NMR resonances, unique to the 1-deoxyglucosamine adduct (i.e., not evident in the glucosamine adduct glyclauxin B1 (**10**)) due to increased rotational freedom about the C-2″/N-2 bond. The glyclauxins proved to be chemically labile, with facile transformations (−MeOH) from the natural product glyclauxins D (**5**) to A (**2**), and C (**4**) to B (**3**), as well as the semisynthetic glyclauxins C1 (**9**) to B1 (**10**). Despite demonstrating a capacity to transform during handling and storage, chemical analysis of fresh CMB-MW102 culture extracts detected **2**−**6** and confirmed their status as natural products. Noting a propensity to form adducts with natural

Scheme 2. Synthesis of 1-Deoxy-D-glucosamine HCl Salt (11) from D-Acetylglucosamine[a]

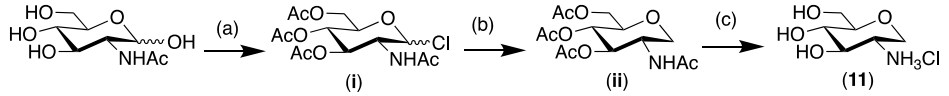

[a]Conditions: (a) acetyl chloride, 16 h, rt; (b) Bu_3SnH, AIBN, inert atmosphere, 120 °C, 1.5 h; (c) 2.5 M HCl, reflux, 4 h.

https://doi.org/10.1021/acs.jnatprod.2c01069
J. Nat. Prod. XXXX, XXX, XXX−XXX

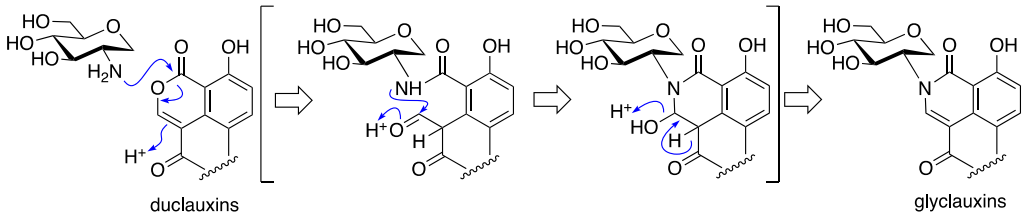

Figure 3. Proposed mechanism for the transformation of duclauxins to glyclauxins.

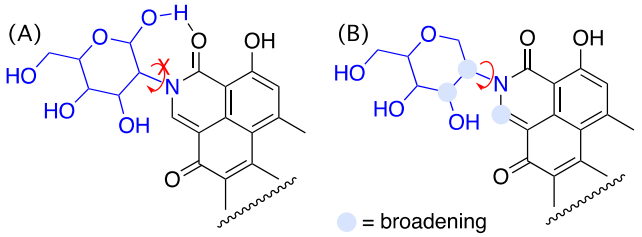

Figure 4. H-bonding in (A) glucosamine adducts restricts rotational freedom, while (B) its absence in 1-deoxyglucosamine adducts allows for increased rotational freedom that facilitates selected NMR resonance broadening.

Scheme 3. A Plausible Biogenetic Relationship Linking Duclauxin (1) with the Glyclauxins, Talauxins, Duclauxamides, and Bacillisporin H, Where Selected Transformations May Be Enzymatic or Nonenzymatic

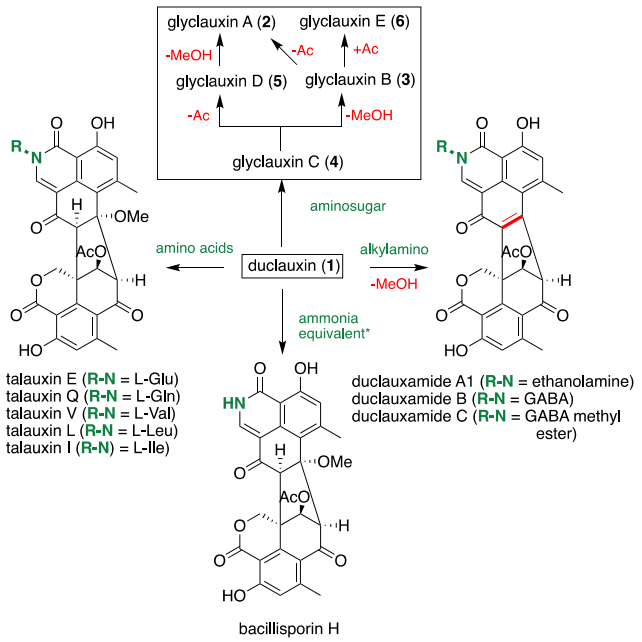

*Potentially sourced from ammonia salts in the culture media.

amines, we propose a biogenetic relationship linking all members of the extended duclauxin structure class. Finally, the discovery of glyclauxins as adducts of 1-deoxy-D-glucosamine (**11**) provides the first indication that this deoxyaminosugar exists naturally.

EXPERIMENTAL SECTION

General Experimental Procedures. Chiroptical measurements ($[\alpha]_D$) were obtained on a JASCO P-1010 polarimeter in a 100 × 2 mm cell at 20.5 °C. NMR spectra were obtained on a Bruker Avance DRX600 spectrometer, in the solvents indicated and referenced to residual signals (δ_H 2.50 and δ_C 39.5 for DMSO-d_6; δ_H 8.74 and δ_C 150.3 for pyridine-d_5; δ_H 7.26 and δ_C 77.0 for $CDCl_3$) in deuterated solvents. Electrospray ionization mass spectra (ESIMS) were acquired using an Agilent 1100 Series separation module equipped with an Agilent 1100 Series LC/MS mass detector in both positive and negative ion modes under the following conditions (Agilent Zorbax SB-C_8 5 μm, 150 × 4.6 mm column, with a 15 min gradient elution at 1.0 mL/min from 90% H_2O/MeCN to 100% MeCN with an isocratic 0.05% HCO_2H modifier). Ultra-high-performance liquid chromatograms (UPLC) were obtained on an Agilent 1290 Infinity UPLC system composed of a 1290 Infinity quaternary pump, thermostat, autosampler, and diode array detector (Agilent Zorbax SB-C_8 RRHD 1.8 μm, 50 × 2.1 mm column, with a 2.50 min gradient elution at 0.417 mL/min from 90% H_2O/MeCN to 100% MeCN with an isocratic 0.01% TFA modifier). High-resolution ESIMS measurements were obtained on a Bruker micrOTOF mass spectrometer by direct infusion in MeCN at 3 μL/min using sodium formate clusters as an internal calibrant. Preparative and semipreparative HPLC were performed using an Agilent 1100 Series diode array and/or multiple wavelength detectors and Agilent 1100 Series fraction collector. Molecular modeling, including energy-minimized structures, was performed using Chem3D Ultra version 20 (PerkinElmer) with MM2 energy minimization.

Collection and Taxonomy of CMB-MW102. The fungus CMB-MW102 was isolated from the surface of a mud dauber wasp larvae inside the wasp nest, on potato dextrose (PD) agar and incubated at 26 °C for 14 days. The colonies first appear white, turning to yellow with time (Figure S1). Genomic DNA was extracted from the mycelia of a static broth culture of corresponding organism using the DNeasy plant mini kit (Qiagen), as per the manufacturer's protocol. The 18S rRNA genes were amplified by PCR using the universal primers ITS-1 (5′-TCCGTAGGTGAACCTGCGG-3′) and ITS-4 (5′-TCCTCCGCTTATTGATATGC-3′) purchased from Sigma-Aldrich. The PCR mixture (50 μL) contained genomic DNA (2 μL, 20−40 ng), EmeraldAmpn GT PCR master mix (2× Premix) (25 μL), primer (0.2 μM, each), and H_2O (up to 50 μL). PCR was performed using the following conditions: initial denaturation at 95 °C for 2 min, 30 cycles in series of 95 °C for 20 s (denaturation), 56 °C for 20 s (annealing), and 72 °C for 30 s (extension), followed by one cycle at 72 °C for 5 min. PCR products were purified with a PCR purification kit (Qiagen) and sequenced. BLAST analysis (NCBI database) showed that the amplified 18S rRNA sequence (GenBank accession number OP854679) has 99% identity with *Talaromyces stipitatus* strain CBS 130166 (Figures S2 and S3).

Scale-up Cultivation and Compound Purification. The fungus CMB-MW102 was cultivated on PD agar plates (×100), incubated at 26 °C for 14 d. Following incubation, the agar was diced (~1.5 cm^2) and extracted with EtOAc (2 × 600 mL) and the combined organic phase concentrated *in vacuo* at 40 °C to yield an extract (700.4 mg), which was further partitioned between hexane (2 × 50 mL) and 90% aqueous MeOH (50 mL) and concentrated *in vacuo* to yield hexane (104.0 mg) and MeOH (596.4 mg) solubles. The MeOH solubles were fractionated by preparative HPLC chromatography (Phenomenex Luna-C_8 column, 9.4 × 250 mm, 10 μm, 20 mL/min gradient elution from 90% H_2O/MeCN to MeCN over 30 min with constant 0.01% TFA as a modifier) to yield 13 fractions. Fraction 4 (16.1 mg) was subjected to semipreparative

https://doi.org/10.1021/acs.jnatprod.2c01069
J. Nat. Prod. XXXX, XXX, XXX−XXX

HPLC (Agilent Zorbax SB-C_3 column, 9.4 mm × 25 cm, 5 μm, 3 mL/min isocratic elution over 35 min with 70% H_2O/MeCN) to yield glyclauxin D (**5**) (2.4 mg, 0.68%). Fraction 5 (16.3 mg) was subjected to semipreparative HPLC (Agilent Zorbax SB-C_3 column, 9.4 mm × 25 cm, 5 μm, 3 mL/min isocratic elution with 70% H_2O/MeCN over 40 min) to yield glyclauxin A (**2**) (3.5 mg, 0.99%). Fraction 6 (15.0 mg) was subjected to semipreparative HPLC (Agilent Zorbax SB-C3 9.4 mm × 25 cm, 5 μm, 3 mL/min isocratic elution over 40 min with 65% H_2O/MeCN) to yield glyclauxin C (**4**) (3.0 mg, 0.85%). Fraction 8 (20.1 mg) was subjected to semipreparative HPLC (Agilent Zorbax SB-C_3 column, 9.4 mm × 25 cm, 5 μm, 3 mL/min isocratic elution over 35 min with 60% H_2O/MeCN) to yield glyclauxin B (**3**) (3.0 mg, 0.85%). Fraction 9 (12.1 mg) was subjected to semipreparative HPLC (Agilent Zorbax SB-C_3 column, 9.4 mm × 25 cm, 5 μm, 3 mL/min gradient elution over 40 min with 59% to 57% H_2O/MeCN) to yield glyclauxin E (**6**) (1.4 mg, 0.4%). Fraction 10 consisted of duclauxin (**1**) (40.0 mg, 11.35%) (Scheme S1). (Note: % yields estimated on a mass-to-mass basis against the weight of the EtOAc extract.)

Duclauxin (1): brown crystals; $[\alpha]^{21}_D$ +227 (*c* 0.076, MeOH); NMR (600 MHz, DMSO-d_6) see Table S1 and Figures S5 and S6; ESI(+)MS *m/z* 547 $[M + H]^+$; HRESI(+)MS *m/z* 569.1061 $[M + Na]^+$ (calcd for $C_{29}H_{22}O_{11}Na$, 569.1054) (Figure S7).

Glyclauxin A (2): orange powder; $[\alpha]^{21}_D$ −286 (*c* 0.110, MeOH); NMR (600 MHz, DMSO-d_6) see Tables 1, 2, and S2 and Figures S8−S12; NMR (600 MHz, pyridine-d_5) see Table S3 and Figures S13−S18; ESI(+)MS *m/z* 618 $[M + H]^+$; HRESI(+)MS *m/z* 640.1433 $[M + Na]^+$ (calcd for $C_{32}H_{27}NO_{12}Na$, 640.1425) (Figure S19).

Glyclauxin B (3): orange powder; $[\alpha]^{21}_D$ −374 (*c* 0.156, MeOH); NMR (600 MHz, DMSO-d_6) see Tables 1, 2, and S4 and Figures S20−S24; ESI(+)MS *m/z* 660 $[M + H]^{+;}$ HRESI(+)MS *m/z* 682.1539 $[M + Na]^+$ (calcd for $C_{34}H_{29}NO_{13}Na$, 682.1531) (Figure S25).

Glyclauxin C (4): yellow powder; $[\alpha]^{21}_D$ −368 (*c* 0.185, MeOH); NMR (600 MHz, DMSO-d_6) see Tables 1, 2, and S5 and Figures S26−S30; ESI(+)MS *m/z* 692 $[M + H]^+$; HRESI(+)MS *m/z* 714.1792 $[M + Na]^+$ (calcd for $C_{35}H_{33}NO_{14}Na$, 714.1793) (Figure S31).

Glyclauxin D (5): yellow powder; $[\alpha]^{21}_D$ −388 (*c* 0.12, MeOH); NMR (600 MHz, DMSO-d_6) see Tables 2, 3, and S6 and Figures S32−S36; ESI(+)MS *m/z* 650 $[M + H]^+$; HRESI(+)MS *m/z* 672.1714 $[M + Na]^+$ (calcd for $C_{33}H_{31}NO_{13}Na$, 672.1688) (Figure S37).

Glyclauxin E (6): orange powder; $[\alpha]^{21}_D$ −368 (*c* 0.115, MeOH); NMR (600 MHz, DMSO-d_6) see Tables 2, 3, and S7 and Figures S38−S42; ESI(+)MS *m/z* 702 $[M + H]^+$; HRESI(+)MS *m/z* 724.1628 $[M + Na]^+$ (calcd for $C_{36}H_{31}NO_{14}Na$, 724.1637) (Figure S43).

Reaction of Duclauxin (1) with D-Glucosamine. Duclauxin (**1**) (5.0 mg in 0.5 mL of DMSO) was treated with D-glucosamine (5.0 mg in 0.5 mL of water with 2 mg of $NaHCO_3$) and stirred for 4 h at rt, after which the solvent was removed *in vacuo*, and the solid residue was redissolved in MeOH and subjected to semipreparative HPLC chromatography to obtain glyclauxin C1 (**9**) (4.1 mg, 66%). NMR (600 MHz, pyridine-d_5) analysis on **9** showed rapid partial dehydration to glyclauxin B1 (**10**), which over 5 days' storage at rt in pyridine-d_5 resulted in quantitative conversion to glyclauxin B1 (**10**): orange powder; $[\alpha]^{21}_D$ −429 (*c* 0.066, MeOH); NMR (600 MHz, pyridine-d_5) see Table S8 and Figures S44−S48; NMR (600 MHz, DMSO-d_6) see Figures S67 and S68; ESI(+)MS *m/z* 698.1512 $[M + Na]^+$ (calcd for $C_{34}H_{29}NO_{14}Na$, 698.1480) (Figure S49).

Synthesis of 1-Deoxy-D-glucosamine (11). *3,4,6-Tri-O-acetyl-1-chloro-1-deoxy-N-acetylglucosamine (i).* *N*-Acetylglucosamine (1.00 g, 4.52 mmol) was stirred vigorously with acetyl chloride (10 mL) under N_2 for 16 h at rt, after which CH_2Cl_2 (100 mL) was added and the resulting mixture was stirred with saturated $NaHCO_3$ (50 mL). The resulting organic layer was dried over anhydrous Na_2SO_4, filtered, concentrated *in vacuo*, and purified by flash silica column chromatography (100% hexane to 50% EtOAc/hexane) to yield **i**: colorless sticky solid (670 mg, 40%); ^1H NMR (400 MHz, $CDCl_3$) δ_H 6.17 (d, *J* 3.6 Hz, H-1), 5.96 (d, *J* 8.7 Hz, NH), 5.31 (dd, *J* 10.3, 9.5 Hz, H-4), 5.18 (dd, *J* 10.0, 9.5 Hz, H-3), 4.52 (ddd, *J* 10.6, 8.7, 3.6 Hz, H-2), 4.32−4.23 (m, H-5 and H-6a), 4.11 (d, *J* 10.4 Hz, H-6b), 2.08 (s, OCOC$\underline{H}_3$), 2.03 (s, 2 × OCOC$\underline{H}_3$), 1.96 (s, OCOC$\underline{H}_3$); ^1H NMR data are in agreement with those reported by Paiotta et al.;[18] HRESI(+)MS *m/z* 388.0786 $[M + Na]^+$ (calcd for $C_{14}H_{20}ClNO_8Na$, 388.0770).

2-Acetamido-3,4,6-tri-O-acetyl-1,5-anhydro-2-deoxy-D-glucopyranose (ii). Bu_3SnH (1 M in cyclohexane, 0.16 mL, 0.16 mmol, 1.2 equiv) and AIBN (0.2 M in toluene, 0.068 mL, 0.014 mmol, 0.1 equiv) were added to a suspension of **i** (50 mg, 0.14 mmol) in dry toluene (3 mL) under an inert atmosphere and degassed using a freeze, pump, and thaw technique (4 × 2 min). The resulting mixture was stirred at 120 °C for 1.5 h, after which it was evaporated *in vacuo* and the residue purified by semipreparative HPLC (Agilent Zorbax XDB C_8, 9.4 mm × 25 cm, 5 μm, 15 min 3 mL/min gradient elution from 15% MeCN/H_2O to 20% MeCN/H_2O) to yield **ii** (7 mg, 16%): ^1H NMR (600 MHz, $CDCl_3$) δ_H 5.67 (d, *J* 7.1 Hz, NH), 5.08 (dd, *J* 9.6, 9.6 Hz, H-4), 4.94 (dd, *J* 10.0, 9.6 Hz, H-3), 4.22−4.17 (m, H-2, H-6a, H-1a), 4.13 (dd, *J* 12.3, 2.3 Hz, H-1b), 3.54 (m, H-5), 3.15 (dd, *J* 12.5, 12.5 Hz, H-6b), 2.10 (s, OCOC$\underline{H}_3$), 2.07 (s, OCOC$\underline{H}_3$), 2.04 (s, OCOC$\underline{H}_3$), 1.94 (s, NHCOC$\underline{H}_3$); ^{13}C NMR (150 MHz, $CDCl_3$) δ_C 172.2 (CO), 170.8 (CO), 170.2 (CO), 169.3 (CO), 76.6 (C-5), 74.2 (C-3), 68.2 (C-4), 68.0 (C-1), 62.3 (C-6), 50.6 (C-2), 23.2 (NHCO$\underline{C}H_3$), 20.79 (OCO$\underline{C}H_3$), 20.76 (OCO$\underline{C}H_3$), 20.6 (OCO$\underline{C}H_3$); ^1H and ^{13}C NMR data are in agreement with those reported by Paiotta et al.;[18] HRESI(+)MS *m/z* 354.1180 $[M + Na]^+$ (calcd for $C_{14}H_{21}NO_8Na$, 354.1159).

1-Deoxy-D-glucosamine (11). The acetylated sugar **ii** (4.5 mg, 0.014 mmol) was dissolved in 2.5 M HCl (2.0 mL) and stirred for 4 h at 110 °C, after which the reaction mixture was lyophilized to give **11** (2.7 mg, 100%): colorless oil; $[\alpha]^{22}_D$ 15 (*c* 0.10, MeOH); ^1H NMR (600 MHz, D_2O) δ_H 4.17 (dd, *J* 11.4, 5.0 Hz, H-1a), 3.88 (dd, *J* 12.4, 1.7 Hz, H-6a), 3.71 (dd, *J* 12.4, 5.6 Hz, H-6b), 3.63 (dd, *J* 9.6, 9.4 Hz, H-4), 3.54 (dd, *J* 11.3, 11.3 Hz, H-1b), 3.44 (dd, *J* 9.5. 9.0 Hz, H-3), 3.38 (ddd, *J* 9.6, 5.6, 1.7 Hz, H-5), 3.28 (ddd, *J* 10.8, 10.8, 5.0 Hz, H-2); ^{13}C NMR (150 MHz, D_2O) δ_C 81.0 (C-5), 74.0 (C-4), 70.1 (C-3), 65.9 (C-1), 61.0 (C-6), 51.7 (C-2); ^1H and ^{13}C NMR data are in agreement with those reported by Neumann et al.;[19] HRESI(+)MS *m/z* 349.1581 $[2M + Na]^+$ (calcd for $C_{12}H_{26}N_2O_8Na$, 349.1581).

Transformation of Duclauxin (1) to Glyclauxin B (3). A solution of **11** (2.5 mg) in H_2O (250 μL), sodium bicarbonate (1.3 mg in 130 μL of H_2O, 12.5 μmol), and duclauxin (**1**) (6.0 mg in 600 μL of DMSO, 12.5 μmol) was stirred at rt for 4 d, after which the solvent was removed *in vacuo*, and the residue (8.6 mg) purified by semipreparative HPLC (Agilent Zorbax XDB C_8, 9.4 mm × 25 cm, 5 μm, 3 mL/min isocratic elution over 13 min with 60% H_2O/MeCN with a 0.01% TFA modifier) to yield glyclauxin B (**3**) (2.3 mg, 32%): orange powder; $[\alpha]^{24}_D$ −344 (*c* 0.100, MeOH); NMR (600 MHz, DMSO-d_6) see Figures S58 and S59; HRESI(+)MS *m/z* 660.1712 $[M + H]^+$ (calcd for $C_{34}H_{30}NO_{13}$, 660.1712).

Detection of Glyclauxins in CMB-MW102 Mycelium and Culture Broth. PD broth cultures (80 mL) inoculated with CMB-MW102 were incubated for 14 days at 26 °C, after which the mycelium and culture broth were separated and individually extracted with EtOAc, and the organic phases were dried under N_2 at rt and immediately subjected to quantitative UPLC-DAD chromatography (Agilent Zorbax SB-C_8 RRHD 1.8 μm, 50 × 2.1 mm column, 0.417 mL/min gradient elution over 2.50 min from 90% H_2O/MeCN to 100% MeCN with an isocratic 0.01% TFA/MeCN modifier) (Figure S62).

Cytotoxicity (MTT) Assay. Adherent SW620 (susceptible human colorectal carcinoma) and NCI-H460 (adherent epithelial like, human lung carcinoma) were cultured in Roswell Park Memorial Institute (RPMI) 1640 medium. All cells were cultured as adherent monolayers in flasks supplemented with 10% fetal bovine serum, 2 mM L-glutamine, 100 unit/mL penicillin, and 100 μg/mL streptomycin in a humidified 37 °C incubator supplied with 5% CO_2. Briefly, cells were harvested with trypsin and dispensed into 96-well microtiter assay plates at 2000 cells/well, after which they were

https://doi.org/10.1021/acs.jnatprod.2c01069
J. Nat. Prod. XXXX, XXX, XXX−XXX

incubated for 24 h at 37 °C with 5% CO_2 (to allow cells to attach as adherent monolayers). Compounds **1**–**6** were dissolved in 20% DMSO in sterile water (v/v), and aliquots (10 μL) applied to cells with a final concentration of 30 μM. After 48 h of incubation at 37 °C with 5% CO_2 an aliquot (10 μL) of 3-(4,5-dimethylthiazol-2-yl)-2,5-diphenyltetrazolium bromide (MTT) in sterile water (5 mg/mL) was added to each well, and microtiter plates were incubated for a further 3 h at 37 °C with 5% CO_2. After final incubation, the medium was aspirated, and precipitated formazan crystals were dissolved in DMSO (100 μL/well). The absorbance of each well was measured at 600 nm with a POLARstar Omega plate reader (BMG LABTECH) (Figure S63). The negative control was 1% aqueous DMSO, while the positive control was vinblastine (final concentrations 30 μM). All experiments were performed in duplicate from two independent cultures.

Antibacterial Assay. The bacteria to be tested was streaked onto an LB agar plate and incubated at 37 °C for 24 h. One colony was then transferred to fresh LB broth (5 mL) and the cell density adjusted to 10^4–10^5 CFU/mL. Analytes (compounds) to be tested were dissolved in DMSO and diluted with H_2O to a stock solution (600 μM in 20% DMSO), which was serially diluted to give concentrations ranging from 600 to 0.2 μM in 20% DMSO. An aliquot (10 μL) of each dilution was transferred to a 96-well microtiter plate, and freshly prepared microbial broth (190 μL) added to each well to give final analyte concentrations ranging from 30 to 0.01 μM in 1% DMSO. Assay plates were incubated at 37 °C for 24 h, and the optical density of each well was measured spectrophotometrically at 600 nm using a POLARstar Omega plate (BMG LABTECH, Offenburg, Germany). Each analyte was screened against the Gram-negative bacteria *Escherichia coli* ATCC 11775 and the Gram-positive isolate *Staphylococcus aureus* ATCC 25923. Rifampicin and ampicillin were used as positive controls (30 μM in 1% DMSO).

Antifungal Assay. The fungus *Candida albicans* ATCC 10231 was streaked onto an LB agar plate and incubated at 37 °C for 48 h. One colony was then transferred to fresh LB broth (5 mL), and the cell density adjusted to 10^4–10^5 CFU/mL. Analytes (compounds) to be tested were dissolved in DMSO and diluted with H_2O to give a stock solution (600 μM in 20% DMSO), which was serially diluted with 20% DMSO to give concentrations from 600 to 0.2 μM in 20% DMSO. An aliquot (10 μL) of each dilution was transferred to a 96-well microtiter plate, and freshly prepared fungal broth (190 μL) added to each well to give final analyte concentrations ranging from 30 to 0.01 μM in 1% DMSO. The plates were incubated at 37 °C for 24 h, and the optical density of each well was measured spectrophotometrically at 600 nm using a POLARstar Omega plate (BMG LABTECH, Offenburg, Germany). Ketoconazole B was used as a positive control (30 μM in 1% DMSO).

■ ASSOCIATED CONTENT

Supporting Information

The Supporting Information is available free of charge at https://pubs.acs.org/doi/10.1021/acs.jnatprod.2c01069.

Bacterial taxonomy, NMR spectra, and tabulated NMR data (PDF)

■ AUTHOR INFORMATION

Corresponding Author

Robert J. Capon − *Institute for Molecular Bioscience, The University of Queensland, Brisbane, QLD 4072, Australia;* orcid.org/0000-0002-8341-7754; Phone: +61 7 3346 2979; Email: r.capon@uq.edu.au

Authors

Kaumadi Samarasekera − *Institute for Molecular Bioscience, The University of Queensland, Brisbane, QLD 4072, Australia;* orcid.org/0000-0003-1021-4400

Waleed M. Hussein − *Institute for Molecular Bioscience, The University of Queensland, Brisbane, QLD 4072, Australia*

Taizong Wu − *Institute for Molecular Bioscience, The University of Queensland, Brisbane, QLD 4072, Australia*

Angela A. Salim − *Institute for Molecular Bioscience, The University of Queensland, Brisbane, QLD 4072, Australia;* orcid.org/0000-0002-8177-5689

Complete contact information is available at: https://pubs.acs.org/10.1021/acs.jnatprod.2c01069

Author Contributions

K.S., W.M.H., and T.W. contributed equally. R.J.C. conceptualized the research; K.S. carried out the isolation and spectroscopic characterization of compounds and performed the biological assays; K.S., A.A.S., and R.J.C. assigned molecular structures; W.M.H. synthesized compound **11**, T.W. carried out the semisynthesis of **3**, A.A.S. constructed the Supporting Information document; R.J.C. reviewed all data and Supporting Information and drafted the manuscript, with support from all authors. The manuscript was written through contributions of all authors. All authors have given approval to the final version of the manuscript.

Funding

This research was supported in part by The University of Queensland and the Institute for Molecular Bioscience.

Notes

The authors declare no competing financial interest.

■ REFERENCES

(1) Quezada, M.; Shang, Z.; Kalansuriya, P.; Salim, A. A.; Lacey, E.; Capon, R. J. *J. Nat. Prod.* **2017**, *80*, 1192−1195.
(2) Kalansuriya, P.; Quezada, M.; Esposito, B. P.; Capon, R. J. *J. Nat. Prod.* **2017**, *80*, 609−615.
(3) Kalansuriya, P.; Khalil, Z. G.; Salim, A. A.; Capon, R. J. *Tetrahedron Lett.* **2019**, *60*, 151157.
(4) Elbanna, A. H.; Khalil, Z. G.; Bernhardt, P. V.; Capon, R. J. *J. Nat. Prod.* **2021**, *84*, 762−770.
(5) Elbanna, A. H.; Khalil, Z. G.; Capon, R. J. *Molecules* **2021**, *26*, 7144.
(6) Salim, A. A.; Samarasekera, K.; Wu, T.; Capon, R. J. *Org. Lett.* **2022**, *24*, 7328−7333.
(7) Aron, A. T.; Gentry, E. C.; McPhail, K. L.; Nothias, L.-F.; Nothias-Esposito, M.; Bouslimani, A.; Petras, D.; Gauglitz, J. M.; Sikora, N.; Vargas, F.; et al. *Nat. Protoc.* **2020**, *15*, 1954−1991.
(8) Shibata, S.; Ogihara, Y.; Tokutake, N.; Tanaka, O. *Tetrahedron Lett.* **1965**, *6*, 1287−1288.
(9) Shahid, H.; Cai, T.; Wang, Y.; Zheng, C.; Yang, Y.; Mao, Z.; Ding, P.; Shan, T. *Front. Microbiol.* **2021**, *12*, 766440.
(10) Ogihara, Y.; Iitaka, Y.; Shibata, S. *Tetrahedron Lett.* **1965**, *6*, 1289−1290.
(11) Cao, P.; Yang, J.; Miao, C.-P.; Yan, Y.; Ma, Y.-T.; Li, X.-N.; Zhao, L.-X.; Huang, S.-X. *Org. Lett.* **2015**, *17*, 1146−1149.
(12) Ogihara, Y.; Tanaka, O.; Shibata, S. *Tetrahedron Lett.* **1966**, *7*, 2867−2873.
(13) Chaudhary, N. K.; Crombie, A.; Vuong, D.; Lacey, E.; Piggott, A. M.; Karuso, P. *J. Nat. Prod.* **2020**, *83*, 1051−1060.
(14) Elbanna, A. H.; Khalil, Z. G.; Bernhardt, P. V.; Capon, R. J. *Org. Lett.* **2019**, *21*, 8097−8100.
(15) Capon, R. J. *Nat. Prod. Rep.* **2020**, *37*, 55−79.
(16) Dramae, A.; Intaraudom, C.; Bunbamrung, N.; Saortep, W.; Srichomthong, K.; Pittayakhajonwut, P. *Tetrahedron* **2020**, *76*, 130980.
(17) Zang, Y.; Genta-Jouve, G.; Escargueil, A. E.; Larsen, A. K.; Guedon, L.; Nay, B.; Prado, S. *J. Nat. Prod.* **2016**, *79*, 2991−2996.
(18) Paiotta, A.; D'Orazio, G.; Palorini, R.; Ricciardiello, F.; Zoia, L.; Votta, G.; De Gioia, L.; Chiaradonna, F.; La Ferla, B. *Eur. J. Org. Chem.* **2018**, *2018*, 1946−1952.

(19) Neumann, J.; Weingarten, S.; Thiem, J. *Eur. J. Org. Chem.* **2007**, *2007*, 1130−1144.

https://doi.org/10.1021/acs.jnatprod.2c01069
J. Nat. Prod. XXXX, XXX, XXX−XXX